Supplementary Information

Organic Phosphorescence in Pt(II)-Complexes linked to Organic Chromophores for Blue-Emitting Organic Light-Emitting Diodes

Seong Woon Jeong,[1,#] Hyung Joo Lee,[1,2,#] Bum Joon Park,[3] Min-Jong Bong,[1,2] Daehan Lee,[1] Taekyung Kim,[4,*] Chul Hoon Kim,[1,2,*] and Ho-Jin Son[1,2,*]

[1]*Department of Advanced Materials Chemistry, Korea University, Sejong 30019, Republic of Korea.*

[2]*Division of Smart Energy Convergence Engineering, Korea University, Sejong 30019, Republic of Korea.*

[3]*Department of Information Display, Hongik University, Seoul 04066, Republic of Korea.*

[4]*Department of Chemical Engineering, Kyung Hee University, Yongin 17104, Republic of Korea.*

[#]*These authors contributed equally.*

*Corresponding authors:
Ho-Jin Son / hjson@korea.ac.kr
Chul Hoon Kim / chulhoon@korea.ac.kr
Taekyung Kim / taekyung.kim@khu.ac.kr

Contents

Supplementary Methods

Crystal Structure Determination. Single crystals of Pt-Cz and Pt-Np were sealed in glass capillaries under argon and mounted on the diffractometer. Preliminary examination and data collection were performed on a Bruker SMART CCD X-ray diffractometer equipped with a sealed-tube X-ray source (50 kV × 30 mA) using graphite-monochromated Mo *Kα* radiation (λ = 0.71073 Å). Preliminary unit cell constants were determined using a set of 45 narrow-frame (0.3° in ω) scans. A double-pass scanning method was used to exclude the noise. The collected frames were integrated using an orientation matrix determined from the narrow-frame scans. The SMART software package was used for data collection, and SAINT was used for frame integration. The final cell constants were determined by global refinement of the *xyz* centroids of the reflections harvested from the entire data set. Structural solution and refinement were performed using the SHELXTL-PLUS software package. Crystallographic data were deposited with the Cambridge Crystallographic Data Centre as supplementary publications (CCDC-2380466 (Pt-Cz) and CCDC-2381488 (Pt-Np)). Additional crystallographic data are provided in Supplementary Tables 1-5.

Electrochemical measurements. Cyclic voltammetry (CV) experiments were performed in distilled, degassed DCM containing 1 mM sample (Pt(II) complexes or Cz/Np) and 0.1 M tetrabutylammonium perchlorate (TBAP) at RT using an electrochemical analyzer (CH Instruments, CHI660e). A platinum disk (diameter, dia. 1.6 mm), platinum wire, and $Ag/AgNO_3$ (0.1 M) were used as the working, counter, and reference electrodes, respectively. Potential values were calibrated against the ferrocene/ferrocenium ($Fc|Fc^+$) redox couple.

Theoretical calculation. Density functional theory (DFT) calculations were performed using the Gaussian 09 program package. The ground-state geometry was fully optimized at the DFT level using the B3LYP (UB3LYP for triplet calculations) method. The 6-31G(d,p) and LANL2DZ basis sets were applied for non-metal atoms and Pt, respectively. Isodensity plots (contour = 0.03 a.u.) of the frontier orbitals were visualized using the Chem3D Ultra or GaussView 6 programs. Time-dependent DFT (TD-DFT) calculations were performed to evaluate the vertical transition energies and oscillator strengths of the singlet and triplet transitions.

Steady-state optical measurements. Steady-state absorption and photoluminescence spectra were acquired using Logies Cary 5000 and Varian Cary Eclipse instruments, respectively.

Phosphorescence spectra at 77 K were obtained using an intensified charge-coupled device (ICCD, Andor, iStar). The samples were excited by nanosecond third-harmonic-generation laser pulses (355 nm, FWHM of 4.5 ns) from a Q-switched Nd:YAG laser (Continuum, Surelite II-10).[1] Absolute PLQYs were determined using a Quantaurus-QY measurement system (C11347-11, Hamamatsu Photonics) and all samples were excited at 305 nm.

Time-resolved optical measurements. A femtosecond amplifed pulse was were generated using a Ti:sapphire regenerative amplifier system (Spectra Physics, Spitfire Ace). An optical parametric amplifier (Spectra Physics, TOPAS prime) was used to produce the excitation pulse at 320 nm. Time-resolved photoluminescence spectra were measured by using a streak scope (Hamamatsu Photonics, C10627) equipped with a polychromator (Princeton Instruments, Acton SpectroPro SP-2300). A femtosecond transient absorption (TA) spectroscopy system (Ultrafast Systems, Helios) was employed to monitor the excited transient species, as described in detail elsewhere.[2] For the TA measurements, the excitation intensity was adjusted using a continuous variable neutral density filter. The remainder of the amplified pulse was sent through an optical delay line and focused onto a 1 mm water cell to produce a white light continuum as a probe beam, which was directed to the sample cell via a 2.0 mm optical path and detected by a CCD detector. The pump pulse was modulated by a mechanical chopper synchronized to one-half of the laser repetition rate, resulting in a pair of spectra generated with and without the pump, from which, the change in absorption induced by the pump pulse was estimated.

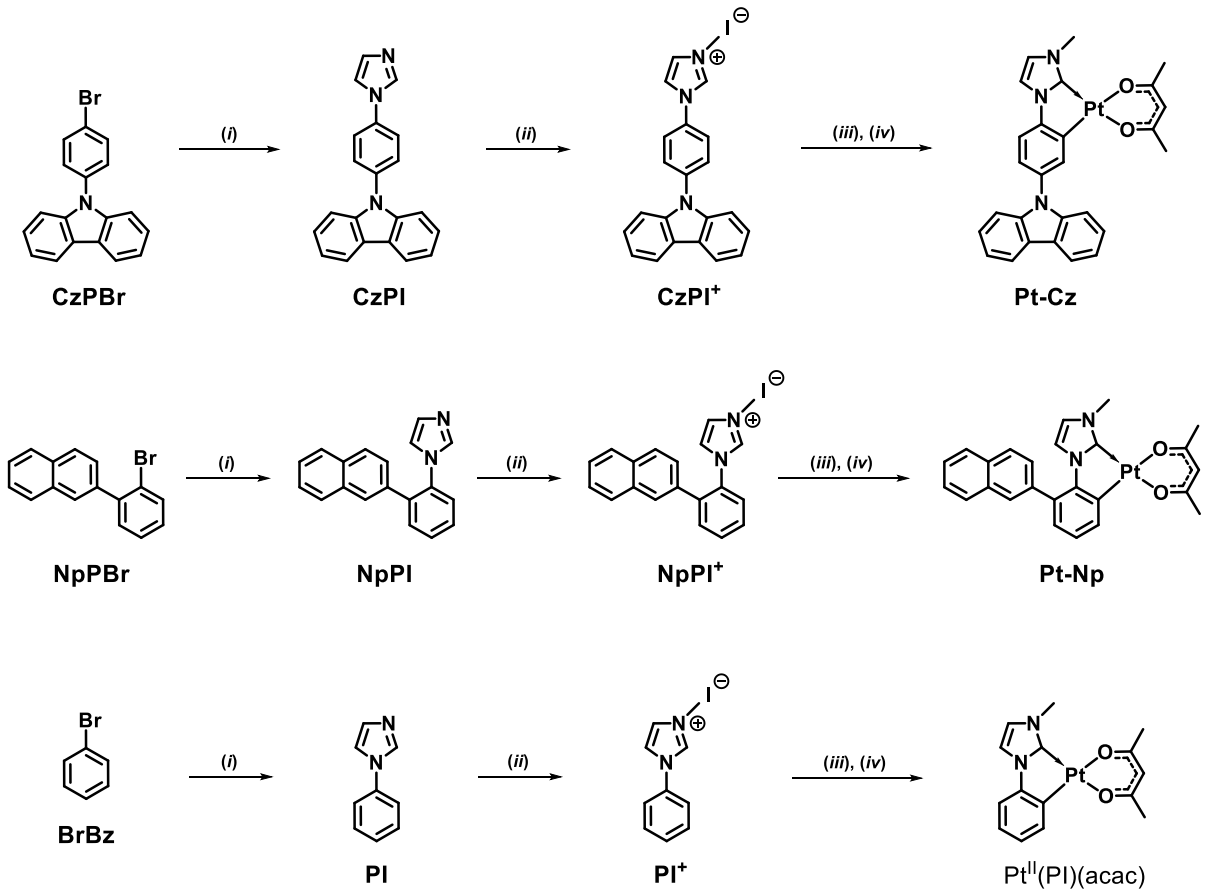

Supplementary Scheme 1. Synthetic route and reaction conditions. Reagents and conditions: (*i*) imidazole, CuI, K_2CO_3, ethylenediamine, dimethylformamide (DMF), N_2, reflux, 160 °C, 72 h; (*ii*) CH_3I, tetrahydrofuran (THF), r.t., 48 h; (*iii*) Ag_2O, 1,4-dioxane, r.t., 16 h and $Pt(COD)Cl_2$, 2-ethoxyethanol, N_2, reflux, 130 °C, 16 h; (i*v*) 2,4-pentanedione (acac), *t*-BuOK, DMF, N_2, reflux, r.t. 16 h and 100 °C 6 h.

Synthesis of $CzPI^+$

Step (*i* & *ii*): 9-(4-bromophenyl)-9*H*-carbazole (CzPBr) (10 g, 31.0 mmol) was dissolved in 200 mL of dimethyl formamide (DMF). Imidazole (4.2 g, 62.0 mmol), copper(I) iodide (CuI, 0.6 g, 3.1 mmol), potassium carbonate (K_2CO_3, 8.6 g, 62.0 mmol), and ethylene diamine (0.6 mL, 9.3 mmol) were added. The mixture was stirred for 72 hours at 160°C. After cooling to room temperature, the solid materials were removed by filtration. The solvent was removed under vacuum, and the remaining substance was dissolved in 150 mL of dichloromethane (DCM). The solution was washed with 25% ammonia solution (25 mL) and 150 mL of water. The two layers were separated, and the organic layer was dried using magnesium sulfate ($MgSO_4$) and filtered. The solvent was evaporated under reduced pressure, and the crude product was purified by column chromatography using ethyl acetate as the eluent. This yielded 8 g (83.3%) of the white solid CzPI. Next, the white solid CzPI (7 g, 22.6 mmol) was dissolved in 140 mL of tetrahydrofuran (THF). Methyl iodide (MeI, 14 mL, 226 mmol) was then added slowly. The mixture was stirred for 48 hours at room temperature. The resulting precipitate was filtered, washed with 100 mL of THF, and dried to obtain the product as a white solid $CzPI^+$, yielding 10 g (97.7%).

^{1}H-NMR ($CDCl_3$, 400 MHz, δ): 10.66 (s, 1H), 8.12 (d, J = 7.5 Hz, 2H), 8.05 (d, J = 8.1 Hz, 2H), 7.79 (d, J = 8.1 Hz, 2H), 7.72 (d, J = 15.6 Hz, 2H), 7.40 (d, J = 3.9 Hz, 4H), 7.32−7.28 (m, 2H), 4.31 (s, 3H).

ESI-MS (*m*/*z*): calcd. for $C_{22}H_{18}IN_3$: 451.0545, found $[M - I]^+$: 324.1514.

Synthesis of $NpPI^+$

Step (*i* & *ii*): 2-(2-Bromophenyl)naphthalene (NpPBr) (8 g, 28.3 mmol) was dissolved in 180 mL of dimethyl formamide (DMF). Imidazole (3.8 g, 56.5 mmol), copper(I) iodide (CuI, 0.5 g, 2.8 mmol), potassium carbonate (K_2CO_3, 7.8 g, 56.5 mmol), and ethylene diamine (0.6 mL, 8.5 mmol) were added to the solution. The mixture was stirred for 72 hours at 160°C. After cooling to room temperature, the insoluble fraction was removed by filtration. The solvent was evaporated under vacuum, and the residue was dissolved in 140 mL of dichloromethane (DCM). The solution was washed with 25% ammonia solution (20 mL) and 140 mL of water. After phase separation, the organic layer was dried using magnesium sulfate ($MgSO_4$) and filtered. The filtrate was evaporated under reduced pressure, and the crude product was purified by column chromatography using ethyl acetate as the eluent, yielding NpPI as a beige solid. Yield: 5 g (65.5%). Next, the beige solid product of 1-(2-(Naphthalen-2-yl)phenyl)-1*H*-imidazole (NpPI) (5 g, 18.5 mmol) was dissolved in 100 mL of tetrahydrofuran (THF), followed by the slow addition of methyl iodide (MeI, 11 mL, 185 mmol). The mixture was stirred for 48 hours at room temperature. The resulting precipitate was filtered, washed with 100 mL of THF, and dried to afford $NpPI^+$ as a white solid. Yield: 7 g (91.8%).

^{1}H-NMR ($CDCl_3$, 400 MHz, δ): 9.41 (s, 1H), 7.94 (t, J = 2.8 Hz, 2H), 7.89 (d, J = 9.2 Hz, 2H), 7.80−7.72 (m, 5H), 7.70 (t, J = 1.6 Hz, 1H), 7.66 (t, J = 1.6 Hz, 1H), 7.59 (m, 2H), 7.25 (dd, J = 8.4, 1.6 Hz,1H), 3.83 (s, 3H).

ESI-MS (*m*/*z*): calcd. for $C_{20}H_{17}IN_2$: 412.0436, found $[M + H]^+$: 310.2161.

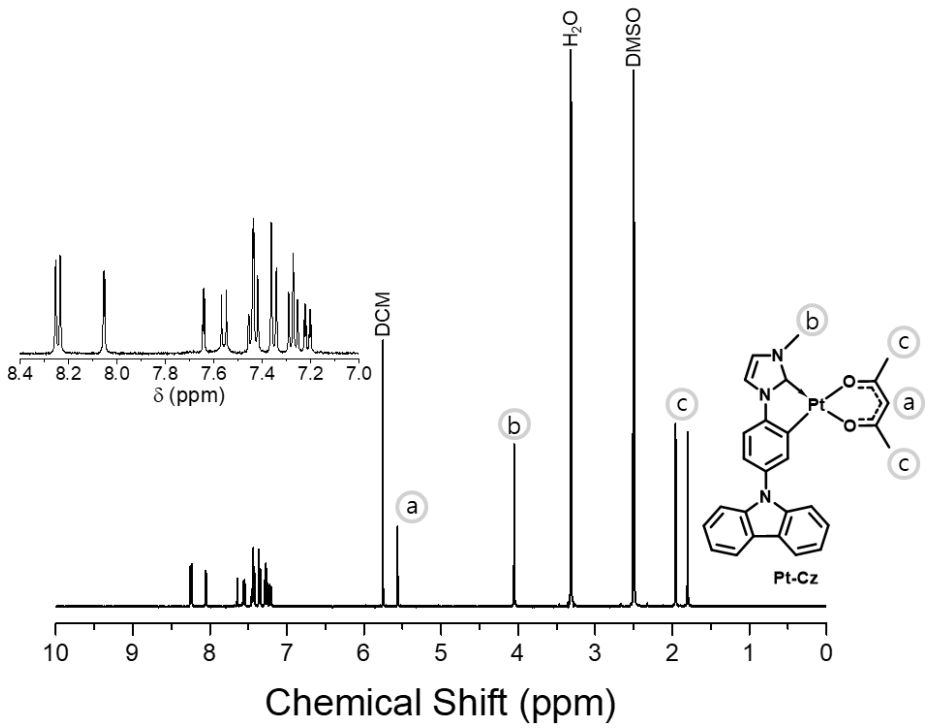

Supplementary Figure 1. ^{1}H-NMR of Pt-Cz.

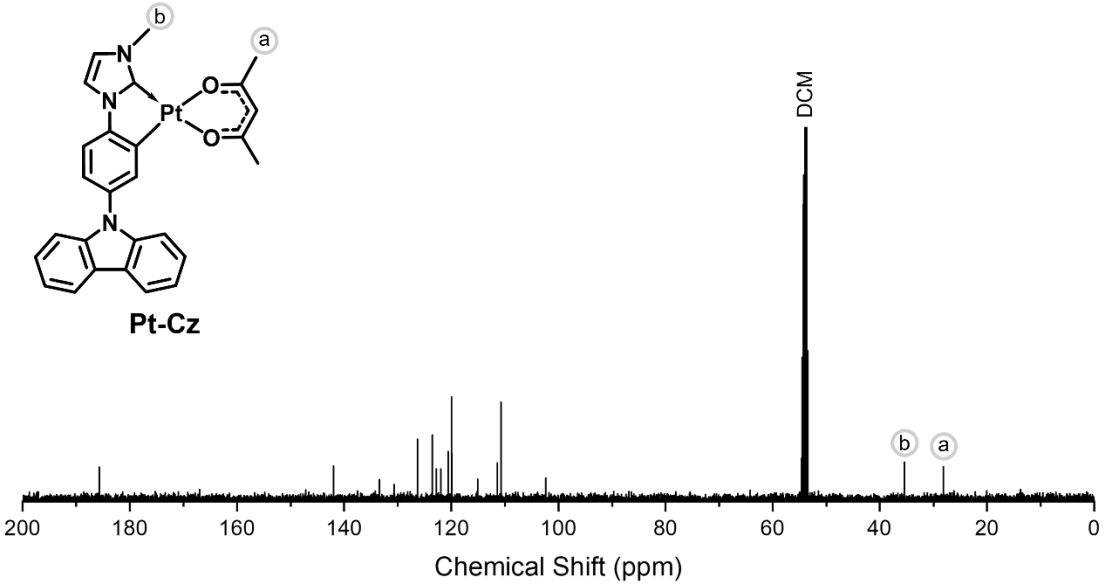

Supplementary Figure 2. ^{13}C-NMR of Pt-Cz.

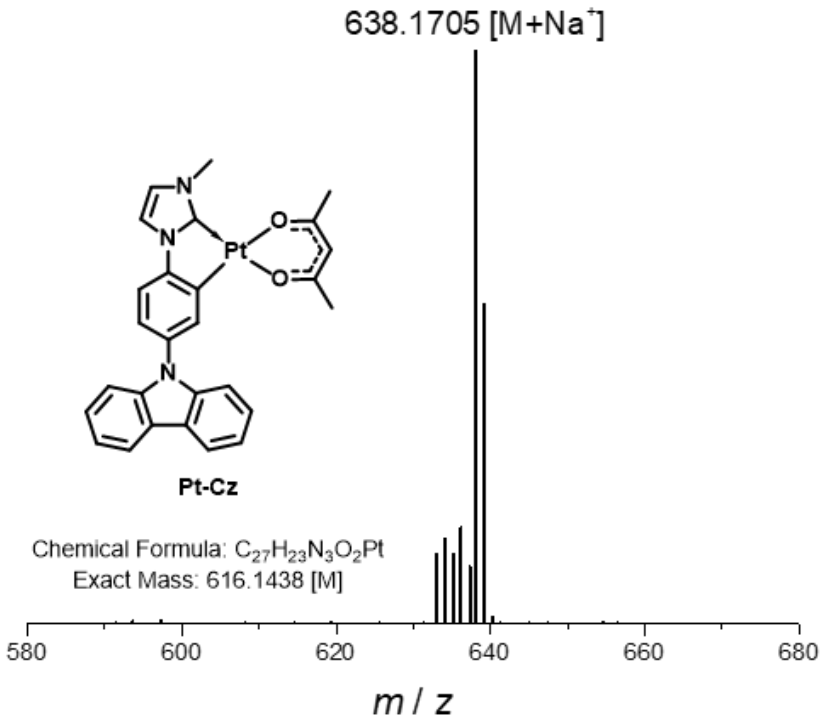

Supplementary Figure 3. ESI-Mass spectrum of Pt-Cz.

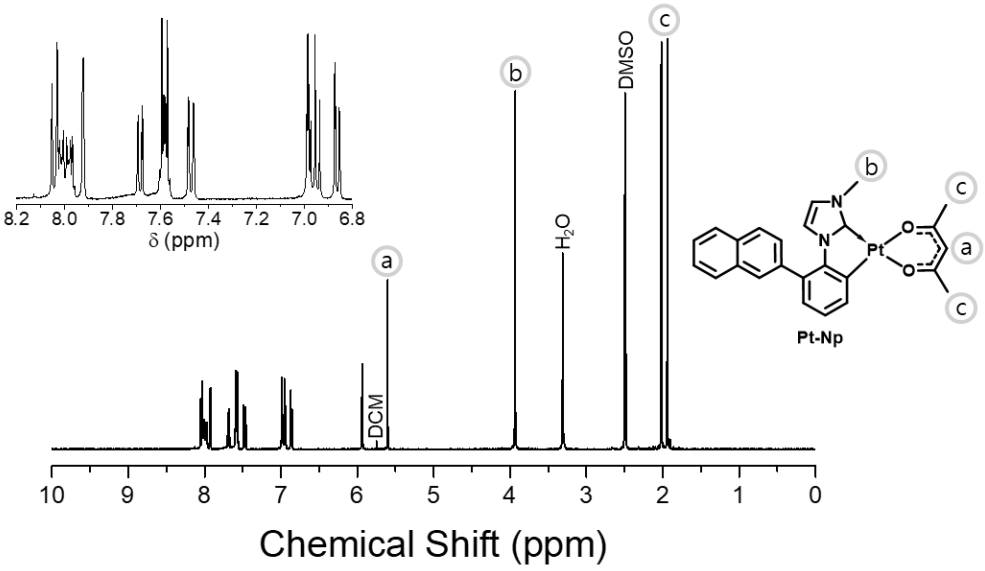

Supplementary Figure 4. ^{1}H-NMR of Pt-Np.

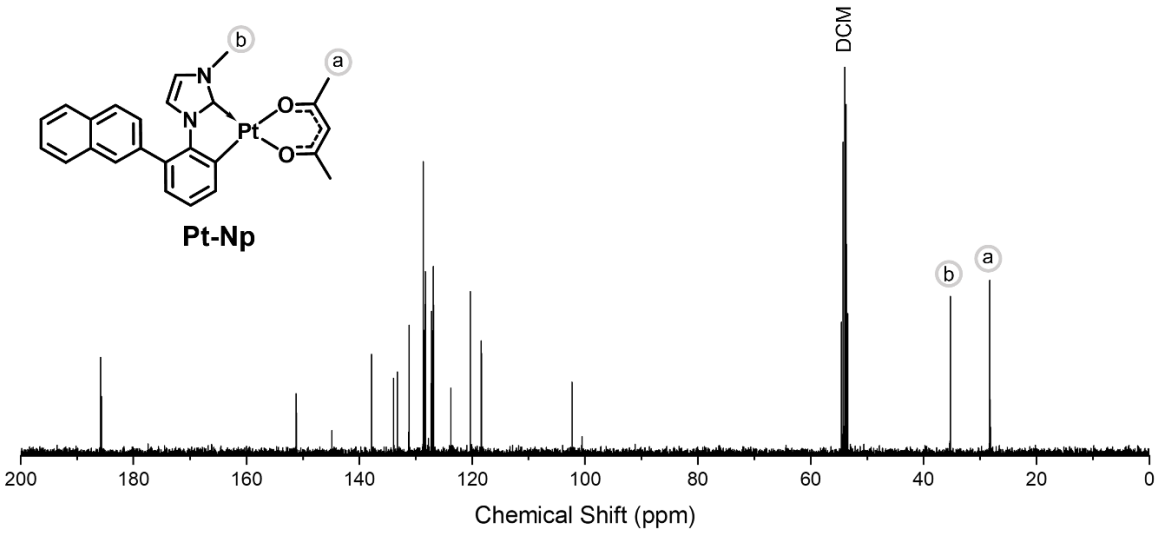

Supplementary Figure 5. ^{13}C-NMR of Pt-Np.

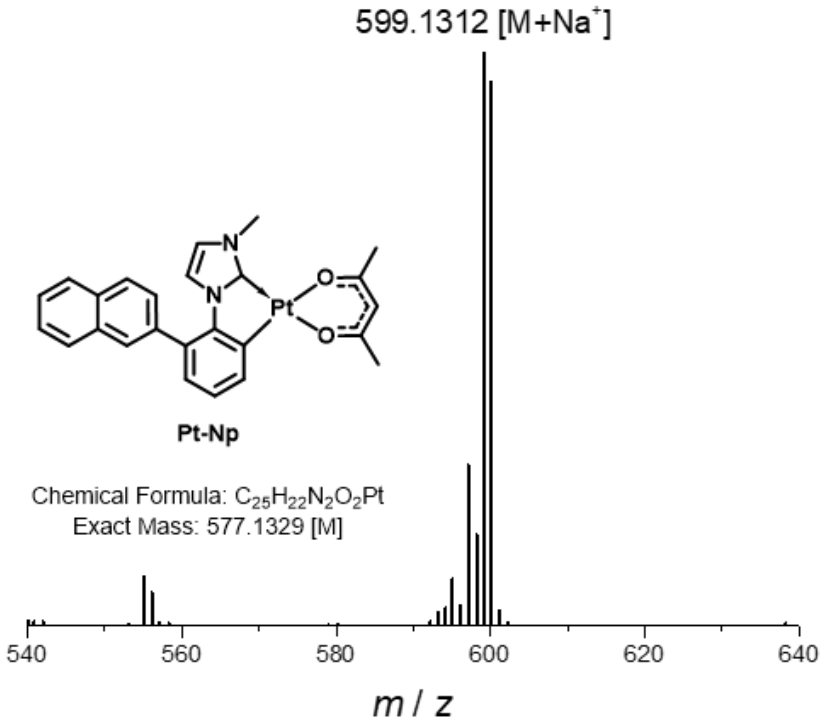

Supplementary Figure 6. ESI-Mass spectrum of Pt-Np.

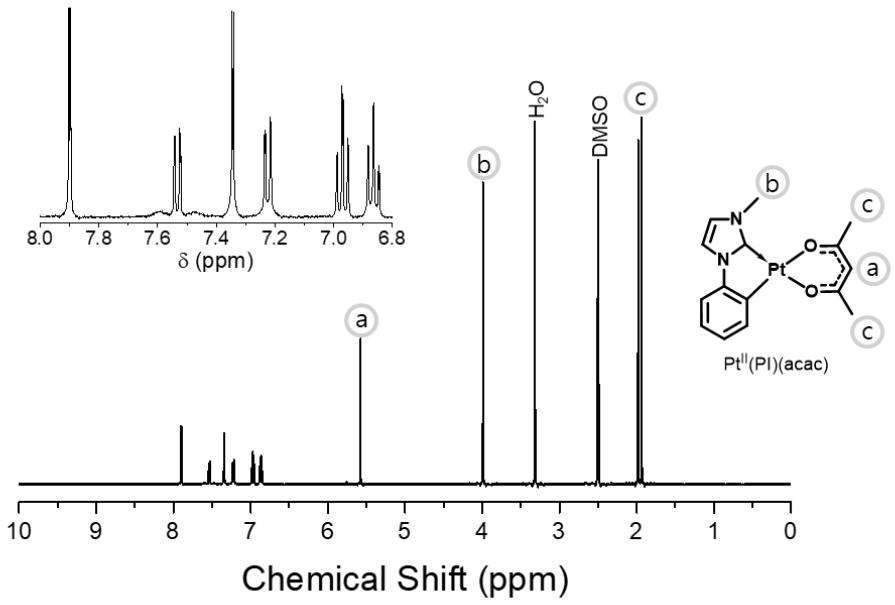

Supplementary Figure 7. ^{1}H-NMR of Pt^{II}(PI)(acac).

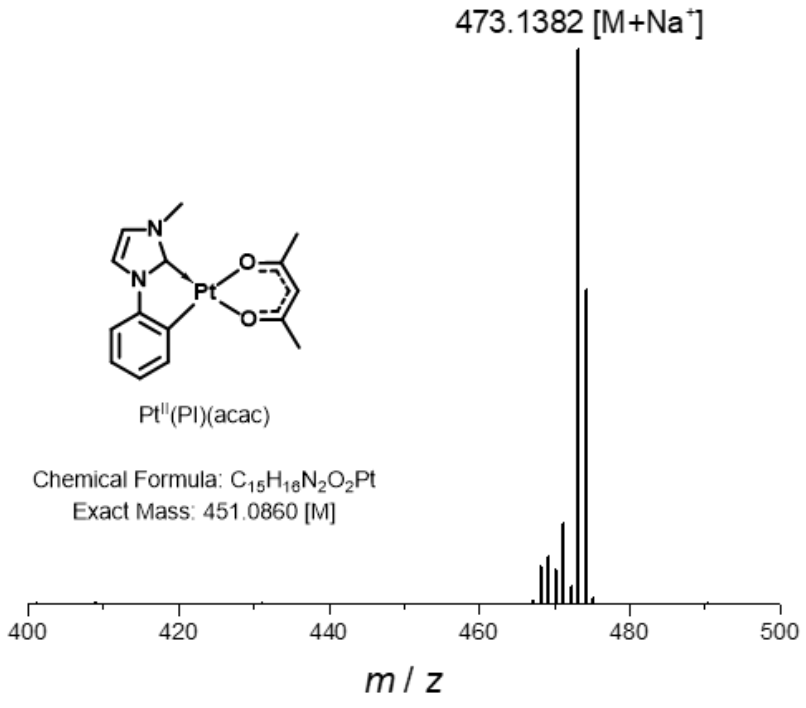

Supplementary Figure 8. ESI-Mass spectrum of Pt^{II}(PI)(acac).

Supplementary Table 1. Crystal data and structure refinement for Pt-Cz and Pt-Np

	Pt-Cz	Pt-Np
Identification code	CCDC 2380466	CCDC 2381488
Empirical formula	C_{27} H_{23} N_3 O_2 Pt	C_{50} H_{44} N_4 O_4 Pt_2
Formula weight	616.57	1154.06
Temperature	296(2) K	296(2) K
Wavelength	0.71073 A	0.71073 A
Crystal system, Space group	Monoclinic, *C*2/*c*	Monoclinic, $P2_1$
Unit cell dimensions	*a* = 24.005(2) Å	*a* = 6.1724(15) Å
	b = 9.1936(9) Å	*b* = 33.358(8) Å
	c = 23.910(2) Å	*c* = 10.513(3) Å
Volume	5259.8(8) $Å^3$	2104.1(9) $Å^3$
Z, D_{calc}	8, 1.557 Mg/m^3	2, 1.822 Mg/m^3
F(000)	2400	1118
Crystal size	0.56 × 0.55 × 0.17 mm	0.30 x 0.20 x 0.02 mm
θ range for data collection	2.314 to 29.221º	1.993 to 25.346º
Limiting indices	$-32 \le h \le 32$, $-12 \le k \le 12$, $-32 \le l \le 32$	$-7 \le h \le 7$, $-40 \le k \le 40$, $-12 \le l \le 12$
Reflections collected / unique	86637 / 7108 [*R*(int) = 0.0925]	27956 / 7393 [R(int) = 0.0941]
Completeness to θ = 25.242	99.7 %	97.6 %
Refinement method	Full-matrix least-squares on F^2	Full-matrix least-squares on F^2
Data / restraints / parameters	7108 / 0 / 301	7393 / 1 / 548
Goodness-of-fit on F^2	1.116	0.972
Final *R* indices [I > 2θ (I)]	$^aR_1$ = 0.0458, ^{b}wR_2 = 0.1384	$^aR_1$ = 0.0439, ^{b}wR_2 = 0.1299
R indices (all data)	$^aR_1$ = 0.0556, ^{b}wR_2 = 0.1466	$^aR_1$ = 0.0510, ^{b}wR_2 = 0.1331
Largest diff. peak and hole	2.530 and −2.170 e.$Å^{-3}$	2.110 and -1.724 e.$Å^{-3}$

$^aR_1 = \sum||F_o|-|F_c||$ (based on reflections with $F_o^2 > 2\sigma F^2$), $^bwR_2 = [\sum[w\ (F_o^2-F_c^2)^2] / \sum[w\ (F_o^2)^2]]^{1/2}$; $w = 1/[\sigma^2\ (F_o^2) + (0.095P)^2]$; $P = [\max(F_o^2, 0) + 2F_c^2]/3$(also with $F_o^2>2\sigma F^2$)

Supplementary Table 2. Bond lengths [Å] for Pt-Cz

Pt(1)-C(6)	1.947(4)	C(9)-H(9)	0.93
Pt(1)-C(10)	1.978(4)	C(10)-C(15)	1.391(7)
Pt(1)-O(1)	2.041(3)	C(10)-C(11)	1.396(7)
Pt(1)-O(2)	2.079(3)	C(11)-C(12)	1.400(8)
O(1)-C(2)	1.267(5)	C(12)-C(13)	1.393(9)
O(2)-C(4)	1.266(8)	C(12)-H(12)	0.93
N(1)-C(6)	1.371(5)	C(13)-C(14)	1.361(8)
N(1)-C(9)	1.373(7)	C(13)-H(13)	0.93
N(1)-C(11)	1.396(7)	C(14)-C(15)	1.390(6)
N(2)-C(6)	1.331(6)	C(15)-H(15)	0.93
N(2)-C(8)	1.417(9)	C(16)-C(17)	1.379(13)
N(2)-C(7)	1.431(8)	C(16)-C(21)	1.413(10)
N(3)-C(16)	1.370(10)	C(17)-C(18)	1.447(14)
N(3)-C(27)	1.393(9)	C(17)-H(17)	0.93
N(3)-C(14)	1.440(7)	C(18)-C(19)	1.337(18)
C(1)-C(2)	1.512(9)	C(18)-H(18)	0.93
C(1)-H(1A)	0.96	C(19)-C(20)	1.365(17)
C(1)-H(1B)	0.96	C(19)-H(19)	0.93
C(1)-H(1C)	0.96	C(20)-C(21)	1.415(12)
C(2)-C(3)	1.387(8)	C(20)-H(20)	0.93
C(3)-C(4)	1.387(10)	C(21)-C(22)	1.434(12)
C(3)-H(3)	0.93	C(22)-C(27)	1.408(9)
C(4)-C(5)	1.515(9)	C(22)-C(23)	1.410(12)
C(5)-H(5A)	0.96	C(23)-C(24)	1.350(18)
C(5)-H(5B)	0.96	C(23)-H(23)	0.93
C(5)-H(5C)	0.96	C(24)-C(25)	1.384(18)
C(7)-H(7A)	0.96	C(24)-H(24)	0.93
C(7)-H(7B)	0.96	C(25)-C(26)	1.379(10)
C(7)-H(7C)	0.96	C(25)-H(25)	0.93
C(8)-C(9)	1.318(10)	C(26)-C(27)	1.388(11)
C(8)-H(8)	0.93	C(26)-H(26)	0.93

Supplementary Table 3. Bond lengths [Å] for Pt-Np

Pt(01)-C(9)	1.97(3)	Pt(02)-C(32)	1.87(3)
Pt(01)-C(1)	2.01(2)	Pt(02)-C(26)	1.95(3)
Pt(01)-O(2)	2.055(19)	Pt(02)-O(3)	2.02(2)
Pt(01)-O(1)	2.06(3)	Pt(02)-O(4)	2.124(18)
O(1)-C(24)	1.34(4)	O(3)-C(47)	1.30(3)
O(2)-C(22)	1.27(3)	O(4)-C(49)	1.23(3)
N(3)-C(9)	1.34(3)	N(1)-C(32)	1.37(3)
N(3)-C(8)	1.38(3)	N(1)-C(34)	1.39(3)
N(3)-C(10)	1.45(3)	N(1)-C(35)	1.49(3)
N(4)-C(7)	1.35(3)	N(2)-C(31)	1.39(3)
N(4)-C(9)	1.37(4)	N(2)-C(33)	1.39(3)
N(4)-C(6)	1.47(3)	N(2)-C(32)	1.41(4)
C(1)-C(6)	1.33(3)	C(26)-C(27)	1.37(3)
C(1)-C(2)	1.42(3)	C(26)-C(31)	1.43(4)
C(2)-C(3)	1.38(3)	C(27)-C(28)	1.38(4)
C(2)-H(2)	0.93	C(27)-H(27)	0.93
C(3)-C(4)	1.35(4)	C(28)-C(29)	1.39(3)
C(3)-H(3)	0.93	C(28)-H(28)	0.93
C(4)-C(5)	1.43(2)	C(29)-C(30)	1.39(2)
C(4)-H(4)	0.93	C(29)-H(29)	0.93
C(5)-C(6)	1.43(3)	C(30)-C(31)	1.37(3)
C(5)-C(11)	1.48(3)	C(30)-C(36)	1.50(3)
C(7)-C(8)	1.34(3)	C(33)-C(34)	1.35(3)
C(7)-H(7)	0.93	C(33)-H(33)	0.93
C(8)-H(8)	0.93	C(34)-H(34)	0.93
C(10)-H(10A)	0.96	C(35)-H(35A)	0.96
C(10)-H(10B)	0.96	C(35)-H(35B)	0.96
C(10)-H(10C)	0.96	C(35)-H(35C)	0.96
C(11)-C(12)	1.36(3)	C(36)-C(37)	1.36(3)
C(11)-C(20)	1.41(3)	C(36)-C(45)	1.43(3)
C(12)-C(13)	1.43(4)	C(37)-C(38)	1.43(3)
C(12)-H(12)	0.93	C(37)-H(37)	0.93
C(13)-C(18)	1.39(3)	C(38)-C(39)	1.38(3)
C(13)-C(14)	1.40(3)	C(38)-C(43)	1.42(3)
C(14)-C(15)	1.34(4)	C(39)-C(40)	1.41(3)
C(14)-H(14)	0.93	C(39)-H(39)	0.93
C(15)-C(16)	1.49(4)	C(40)-C(41)	1.41(4)
C(15)-H(15)	0.93	C(40)-H(40)	0.93
C(16)-C(17)	1.33(4)	C(41)-C(42)	1.28(4)
C(16)-H(16)	0.93	C(41)-H(41)	0.93
C(17)-C(18)	1.47(4)	C(42)-C(43)	1.44(3)
C(17)-H(17)	0.93	C(42)-H(42)	0.93
C(18)-C(19)	1.39(4)	C(43)-C(44)	1.43(3)
C(19)-C(20)	1.42(4)	C(44)-C(45)	1.31(3)
C(19)-H(19)	0.93	C(44)-H(44)	0.93
C(20)-H(20)	0.93	C(45)-H(45)	0.93
C(21)-C(22)	1.46(4)	C(46)-C(47)	1.56(4)
C(21)-H(21A)	0.96	C(46)-H(46A)	0.96

C(21)-H(21B)	0.96	C(46)-H(46B)	0.96
C(21)-H(21C)	0.96	C(46)-H(46C)	0.96
C(22)-C(23)	1.40(4)	C(47)-C(48)	1.32(5)
C(23)-C(24)	1.32(6)	C(48)-C(49)	1.48(5)
C(23)-H(23)	0.93	C(49)-C(50)	1.49(4)
C(24)-C(25)	1.53(5)	C(50)-H(50A)	0.96
C(25)-H(25A)	0.96	C(50)-H(50B)	0.96
C(25)-H(25B)	0.96	C(50)-H(50C)	0.96
C(25)-H(25C)	0.96		

Supplementary Table 4. Angles [°] for Pt-Cz

C(6)-Pt(1)-C(10)	80.48(19)	C(15)-C(10)-Pt(1)	128.4(3)
C(6)-Pt(1)-O(1)	172.25(15)	C(11)-C(10)-Pt(1)	115.0(4)
C(10)-Pt(1)-O(1)	91.79(17)	N(1)-C(11)-C(10)	113.2(5)
C(6)-Pt(1)-O(2)	97.48(16)	N(1)-C(11)-C(12)	123.4(5)
C(10)-Pt(1)-O(2)	175.91(15)	C(10)-C(11)-C(12)	123.4(6)
O(1)-Pt(1)-O(2)	90.20(13)	C(13)-C(12)-C(11)	117.8(5)
C(2)-O(1)-Pt(1)	125.3(3)	C(13)-C(12)-H(12)	121.1
C(4)-O(2)-Pt(1)	124.4(4)	C(11)-C(12)-H(12)	121.1
C(6)-N(1)-C(9)	110.6(4)	C(14)-C(13)-C(12)	119.6(5)
C(6)-N(1)-C(11)	115.5(4)	C(14)-C(13)-H(13)	120.2
C(9)-N(1)-C(11)	133.9(5)	C(12)-C(13)-H(13)	120.2
C(6)-N(2)-C(8)	108.7(5)	C(13)-C(14)-C(15)	122.2(5)
C(6)-N(2)-C(7)	125.3(5)	C(13)-C(14)-N(3)	118.8(5)
C(8)-N(2)-C(7)	125.7(5)	C(15)-C(14)-N(3)	119.0(5)
C(16)-N(3)-C(27)	109.4(6)	C(14)-C(15)-C(10)	120.4(5)
C(16)-N(3)-C(14)	126.1(6)	C(14)-C(15)-H(15)	119.8
C(27)-N(3)-C(14)	124.3(6)	C(10)-C(15)-H(15)	119.8
C(2)-C(1)-H(1A)	109.5	N(3)-C(16)-C(17)	128.2(7)
C(2)-C(1)-H(1B)	109.5	N(3)-C(16)-C(21)	108.0(7)
H(1A)-C(1)-H(1B)	109.5	C(17)-C(16)-C(21)	123.7(8)
C(2)-C(1)-H(1C)	109.5	C(16)-C(17)-C(18)	113.8(12)
H(1A)-C(1)-H(1C)	109.5	C(16)-C(17)-H(17)	123.1
H(1B)-C(1)-H(1C)	109.5	C(18)-C(17)-H(17)	123.1
O(1)-C(2)-C(3)	126.7(5)	C(19)-C(18)-C(17)	123.9(14)
O(1)-C(2)-C(1)	113.7(5)	C(19)-C(18)-H(18)	118
C(3)-C(2)-C(1)	119.6(5)	C(17)-C(18)-H(18)	118
C(4)-C(3)-C(2)	126.6(5)	C(18)-C(19)-C(20)	120.5(11)
C(4)-C(3)-H(3)	116.7	C(18)-C(19)-H(19)	119.8
C(2)-C(3)-H(3)	116.7	C(20)-C(19)-H(19)	119.8
O(2)-C(4)-C(3)	126.5(6)	C(19)-C(20)-C(21)	120.0(11)
O(2)-C(4)-C(5)	115.0(6)	C(19)-C(20)-H(20)	120
C(3)-C(4)-C(5)	118.5(6)	C(21)-C(20)-H(20)	120
C(4)-C(5)-H(5A)	109.5	C(16)-C(21)-C(20)	117.7(10)
C(4)-C(5)-H(5B)	109.5	C(16)-C(21)-C(22)	107.8(6)
H(5A)-C(5)-H(5B)	109.5	C(20)-C(21)-C(22)	134.3(9)
C(4)-C(5)-H(5C)	109.5	C(27)-C(22)-C(23)	119.0(9)
H(5A)-C(5)-H(5C)	109.5	C(27)-C(22)-C(21)	106.0(6)
H(5B)-C(5)-H(5C)	109.5	C(23)-C(22)-C(21)	135.0(8)
N(2)-C(6)-N(1)	105.8(4)	C(24)-C(23)-C(22)	118.9(9)
N(2)-C(6)-Pt(1)	138.4(3)	C(24)-C(23)-H(23)	120.6
N(1)-C(6)-Pt(1)	115.8(3)	C(22)-C(23)-H(23)	120.6
N(2)-C(7)-H(7A)	109.5	C(23)-C(24)-C(25)	121.6(9)
N(2)-C(7)-H(7B)	109.5	C(23)-C(24)-H(24)	119.2
H(7A)-C(7)-H(7B)	109.5	C(25)-C(24)-H(24)	119.2
N(2)-C(7)-H(7C)	109.5	C(26)-C(25)-C(24)	121.6(10)
H(7A)-C(7)-H(7C)	109.5	C(26)-C(25)-H(25)	119.2
H(7B)-C(7)-H(7C)	109.5	C(24)-C(25)-H(25)	119.2
C(9)-C(8)-N(2)	108.2(5)	C(25)-C(26)-C(27)	117.4(9)

C(9)-C(8)-H(8)	125.9	C(25)-C(26)-H(26)	121.3
N(2)-C(8)-H(8)	125.9	C(27)-C(26)-H(26)	121.3
C(8)-C(9)-N(1)	106.6(5)	C(26)-C(27)-N(3)	129.8(6)
C(8)-C(9)-H(9)	126.7	C(26)-C(27)-C(22)	121.5(7)
N(1)-C(9)-H(9)	126.7	N(3)-C(27)-C(22)	108.8(7)
C(15)-C(10)-C(11)	116.5(4)		

Supplementary Table 5. Angles [°] for Pt-Np

C(9)-Pt(01)-C(1)	79.2(12)	H(25B)-C(25)-H(25C)	109.5
C(9)-Pt(01)-O(2)	170.5(10)	C(32)-Pt(02)-C(26)	80.1(13)
C(1)-Pt(01)-O(2)	91.4(9)	C(32)-Pt(02)-O(3)	171.4(11)
C(9)-Pt(01)-O(1)	100.2(8)	C(26)-Pt(02)-O(3)	91.3(10)
C(1)-Pt(01)-O(1)	179.4(11)	C(32)-Pt(02)-O(4)	100.1(9)
O(2)-Pt(01)-O(1)	89.2(8)	C(26)-Pt(02)-O(4)	179.4(10)
C(24)-O(1)-Pt(01)	125(3)	O(3)-Pt(02)-O(4)	88.5(8)
C(22)-O(2)-Pt(01)	126.5(18)	C(47)-O(3)-Pt(02)	126.5(19)
C(9)-N(3)-C(8)	110(2)	C(49)-O(4)-Pt(02)	126.5(18)
C(9)-N(3)-C(10)	126(2)	C(32)-N(1)-C(34)	113(2)
C(8)-N(3)-C(10)	123.8(17)	C(32)-N(1)-C(35)	122(2)
C(7)-N(4)-C(9)	109.8(19)	C(34)-N(1)-C(35)	124.4(18)
C(7)-N(4)-C(6)	136.6(19)	C(31)-N(2)-C(33)	133(2)
C(9)-N(4)-C(6)	113.3(19)	C(31)-N(2)-C(32)	115(2)
C(6)-C(1)-C(2)	121(2)	C(33)-N(2)-C(32)	112(2)
C(6)-C(1)-Pt(01)	117.1(19)	C(27)-C(26)-C(31)	116(2)
C(2)-C(1)-Pt(01)	122.0(18)	C(27)-C(26)-Pt(02)	127(2)
C(3)-C(2)-C(1)	116(2)	C(31)-C(26)-Pt(02)	117.5(17)
C(3)-C(2)-H(2)	122.2	C(26)-C(27)-C(28)	124(2)
C(1)-C(2)-H(2)	122.2	C(26)-C(27)-H(27)	118.2
C(4)-C(3)-C(2)	125(2)	C(28)-C(27)-H(27)	118.2
C(4)-C(3)-H(3)	117.7	C(27)-C(28)-C(29)	119(2)
C(2)-C(3)-H(3)	117.7	C(27)-C(28)-H(28)	120.6
C(3)-C(4)-C(5)	120(2)	C(29)-C(28)-H(28)	120.6
C(3)-C(4)-H(4)	119.8	C(28)-C(29)-C(30)	121(2)
C(5)-C(4)-H(4)	119.8	C(28)-C(29)-H(29)	119.7
C(6)-C(5)-C(4)	115(2)	C(30)-C(29)-H(29)	119.7
C(6)-C(5)-C(11)	127.1(18)	C(31)-C(30)-C(29)	119(2)
C(4)-C(5)-C(11)	118(2)	C(31)-C(30)-C(36)	125.5(17)
C(1)-C(6)-C(5)	124(2)	C(29)-C(30)-C(36)	115(2)
C(1)-C(6)-N(4)	113(2)	C(30)-C(31)-N(2)	128(2)
C(5)-C(6)-N(4)	122.8(19)	C(30)-C(31)-C(26)	122(2)
C(8)-C(7)-N(4)	108(2)	N(2)-C(31)-C(26)	109.0(18)
C(8)-C(7)-H(7)	126	N(1)-C(32)-N(2)	102(2)
N(4)-C(7)-H(7)	126	N(1)-C(32)-Pt(02)	141(2)
C(7)-C(8)-N(3)	107(2)	N(2)-C(32)-Pt(02)	118(2)
C(7)-C(8)-H(8)	126.6	C(34)-C(33)-N(2)	107(2)
N(3)-C(8)-H(8)	126.6	C(34)-C(33)-H(33)	126.6
N(3)-C(9)-N(4)	106(2)	N(2)-C(33)-H(33)	126.6
N(3)-C(9)-Pt(01)	137(2)	C(33)-C(34)-N(1)	107(2)
N(4)-C(9)-Pt(01)	116.9(18)	C(33)-C(34)-H(34)	126.6
N(3)-C(10)-H(10A)	109.5	N(1)-C(34)-H(34)	126.6
N(3)-C(10)-H(10B)	109.5	N(1)-C(35)-H(35A)	109.5
H(10A)-C(10)-H(10B)	109.5	N(1)-C(35)-H(35B)	109.5
N(3)-C(10)-H(10C)	109.5	H(35A)-C(35)-H(35B)	109.5
H(10A)-C(10)-H(10C)	109.5	N(1)-C(35)-H(35C)	109.5
H(10B)-C(10)-H(10C)	109.5	H(35A)-C(35)-H(35C)	109.5
C(12)-C(11)-C(20)	118(2)	H(35B)-C(35)-H(35C)	109.5

C(12)-C(11)-C(5)	120.8(18)	C(37)-C(36)-C(45)	116.0(19)
C(20)-C(11)-C(5)	121(2)	C(37)-C(36)-C(30)	121.5(16)
C(11)-C(12)-C(13)	123.0(18)	C(45)-C(36)-C(30)	122.1(18)
C(11)-C(12)-H(12)	118.5	C(36)-C(37)-C(38)	121.7(17)
C(13)-C(12)-H(12)	118.5	C(36)-C(37)-H(37)	119.2
C(18)-C(13)-C(14)	122(3)	C(38)-C(37)-H(37)	119.2
C(18)-C(13)-C(12)	116(2)	C(39)-C(38)-C(43)	120(2)
C(14)-C(13)-C(12)	121(2)	C(39)-C(38)-C(37)	121.1(19)
C(15)-C(14)-C(13)	120(3)	C(43)-C(38)-C(37)	119.0(17)
C(15)-C(14)-H(14)	120.2	C(38)-C(39)-C(40)	122(2)
C(13)-C(14)-H(14)	120.2	C(38)-C(39)-H(39)	119.2
C(14)-C(15)-C(16)	122(3)	C(40)-C(39)-H(39)	119.2
C(14)-C(15)-H(15)	119.2	C(39)-C(40)-C(41)	115(2)
C(16)-C(15)-H(15)	119.2	C(39)-C(40)-H(40)	122.5
C(17)-C(16)-C(15)	117(3)	C(41)-C(40)-H(40)	122.5
C(17)-C(16)-H(16)	121.5	C(42)-C(41)-C(40)	127(3)
C(15)-C(16)-H(16)	121.5	C(42)-C(41)-H(41)	116.6
C(16)-C(17)-C(18)	123(3)	C(40)-C(41)-H(41)	116.6
C(16)-C(17)-H(17)	118.5	C(41)-C(42)-C(43)	119(2)
C(18)-C(17)-H(17)	118.5	C(41)-C(42)-H(42)	120.7
C(19)-C(18)-C(13)	123(3)	C(43)-C(42)-H(42)	120.7
C(19)-C(18)-C(17)	120(2)	C(38)-C(43)-C(44)	118(2)
C(13)-C(18)-C(17)	116(3)	C(38)-C(43)-C(42)	118(2)
C(18)-C(19)-C(20)	117(2)	C(44)-C(43)-C(42)	124(2)
C(18)-C(19)-H(19)	121.5	C(45)-C(44)-C(43)	118.7(19)
C(20)-C(19)-H(19)	121.5	C(45)-C(44)-H(44)	120.7
C(11)-C(20)-C(19)	122(2)	C(43)-C(44)-H(44)	120.7
C(11)-C(20)-H(20)	119.2	C(44)-C(45)-C(36)	126(2)
C(19)-C(20)-H(20)	119.2	C(44)-C(45)-H(45)	117
C(22)-C(21)-H(21A)	109.5	C(36)-C(45)-H(45)	117
C(22)-C(21)-H(21B)	109.5	C(47)-C(46)-H(46A)	109.5
H(21A)-C(21)-H(21B)	109.5	C(47)-C(46)-H(46B)	109.5
C(22)-C(21)-H(21C)	109.5	H(46A)-C(46)-H(46B)	109.5
H(21A)-C(21)-H(21C)	109.5	C(47)-C(46)-H(46C)	109.5
H(21B)-C(21)-H(21C)	109.5	H(46A)-C(46)-H(46C)	109.5
O(2)-C(22)-C(23)	125(3)	H(46B)-C(46)-H(46C)	109.5
O(2)-C(22)-C(21)	115(3)	O(3)-C(47)-C(48)	128(3)
C(23)-C(22)-C(21)	120(3)	O(3)-C(47)-C(46)	111(3)
C(24)-C(23)-C(22)	129(3)	C(48)-C(47)-C(46)	121(3)
C(24)-C(23)-H(23)	115.6	C(47)-C(48)-C(49)	125(3)
C(22)-C(23)-H(23)	115.6	O(4)-C(49)-C(48)	125(3)
C(23)-C(24)-O(1)	125(4)	O(4)-C(49)-C(50)	115(2)
C(23)-C(24)-C(25)	121(3)	C(48)-C(49)-C(50)	120(3)
O(1)-C(24)-C(25)	114(4)	C(49)-C(50)-H(50A)	109.5
C(24)-C(25)-H(25A)	109.5	C(49)-C(50)-H(50B)	109.5
C(24)-C(25)-H(25B)	109.5	H(50A)-C(50)-H(50B)	109.5
H(25A)-C(25)-H(25B)	109.5	C(49)-C(50)-H(50C)	109.5
C(24)-C(25)-H(25C)	109.5	H(50A)-C(50)-H(50C)	109.5
H(25A)-C(25)-H(25C)	109.5	H(50B)-C(50)-H(50C)	109.5

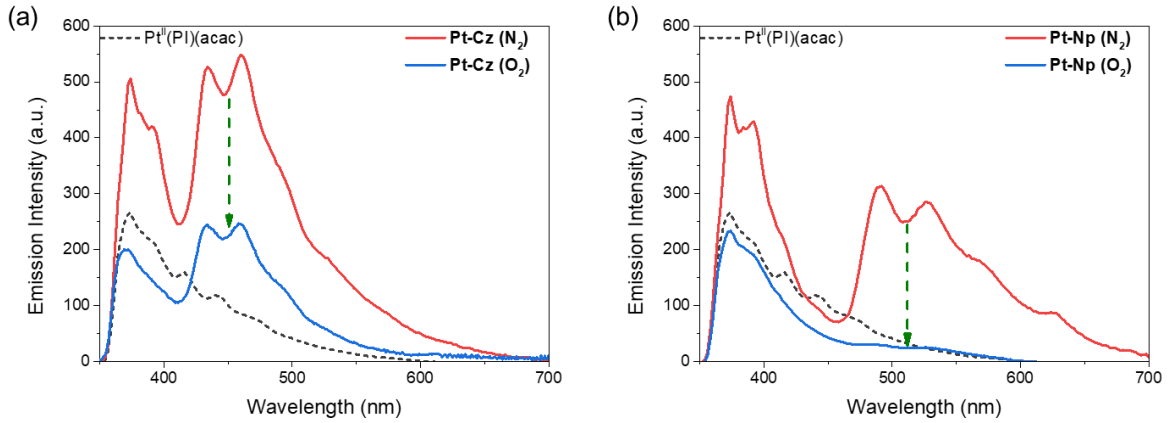

Supplementary Figure 9. PL quenching experiment of Pt(II) complexes. Emission spectra (excited at 320 nm) of (a) Pt-Cz and (b) Pt-Np, measured in nitrogen- and oxygen-saturated DCM at 300 K. The PL spectrum of Pt^{II}(PI)(acac) is included for comparison as a reference sample.

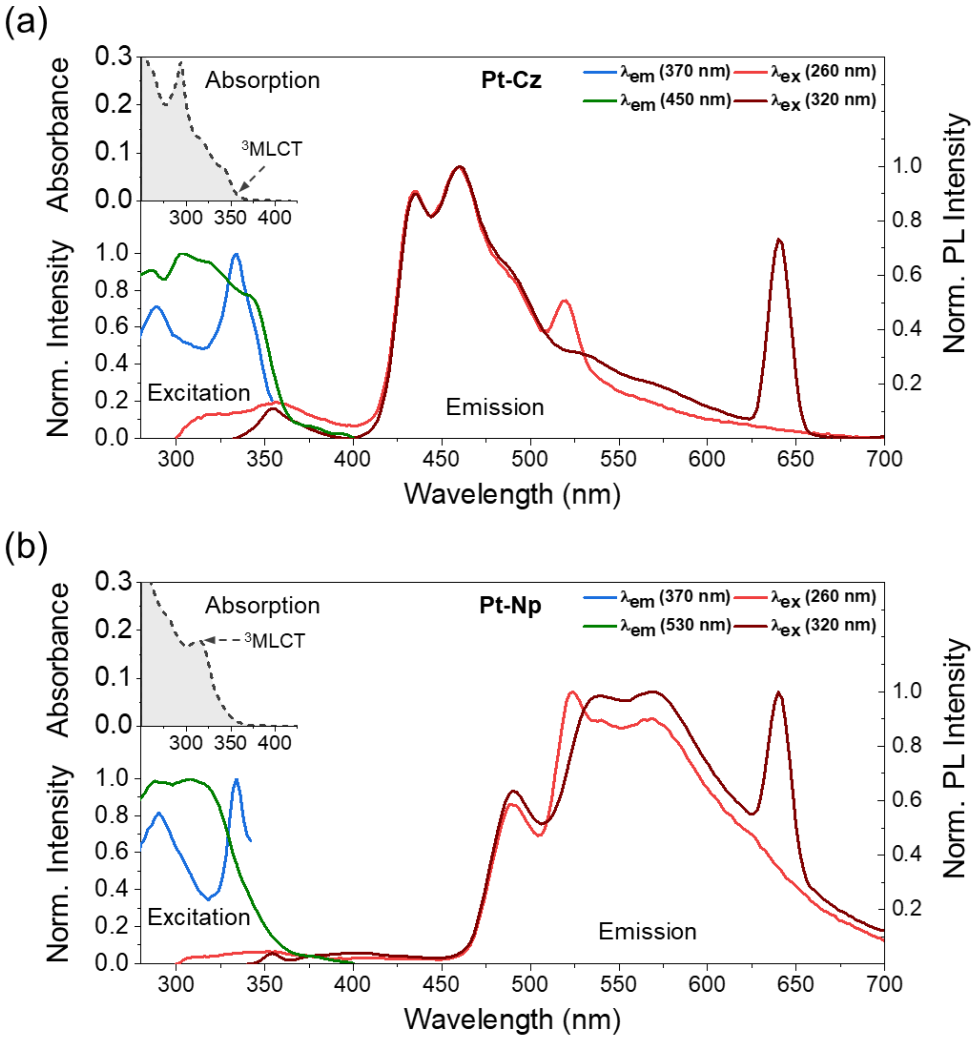

Supplementary Figure 10. Steady-state photophysical properties of Pt(II) complexes. Absorption, emission (excited at 280 nm and 320 nm), and excitation spectra (monitored at two different emission wavelengths) of (a) Pt-Cz and (b) Pt-Np in degassed DCM at 300 K. The asterisk (*) indicates the solvent Raman peak.

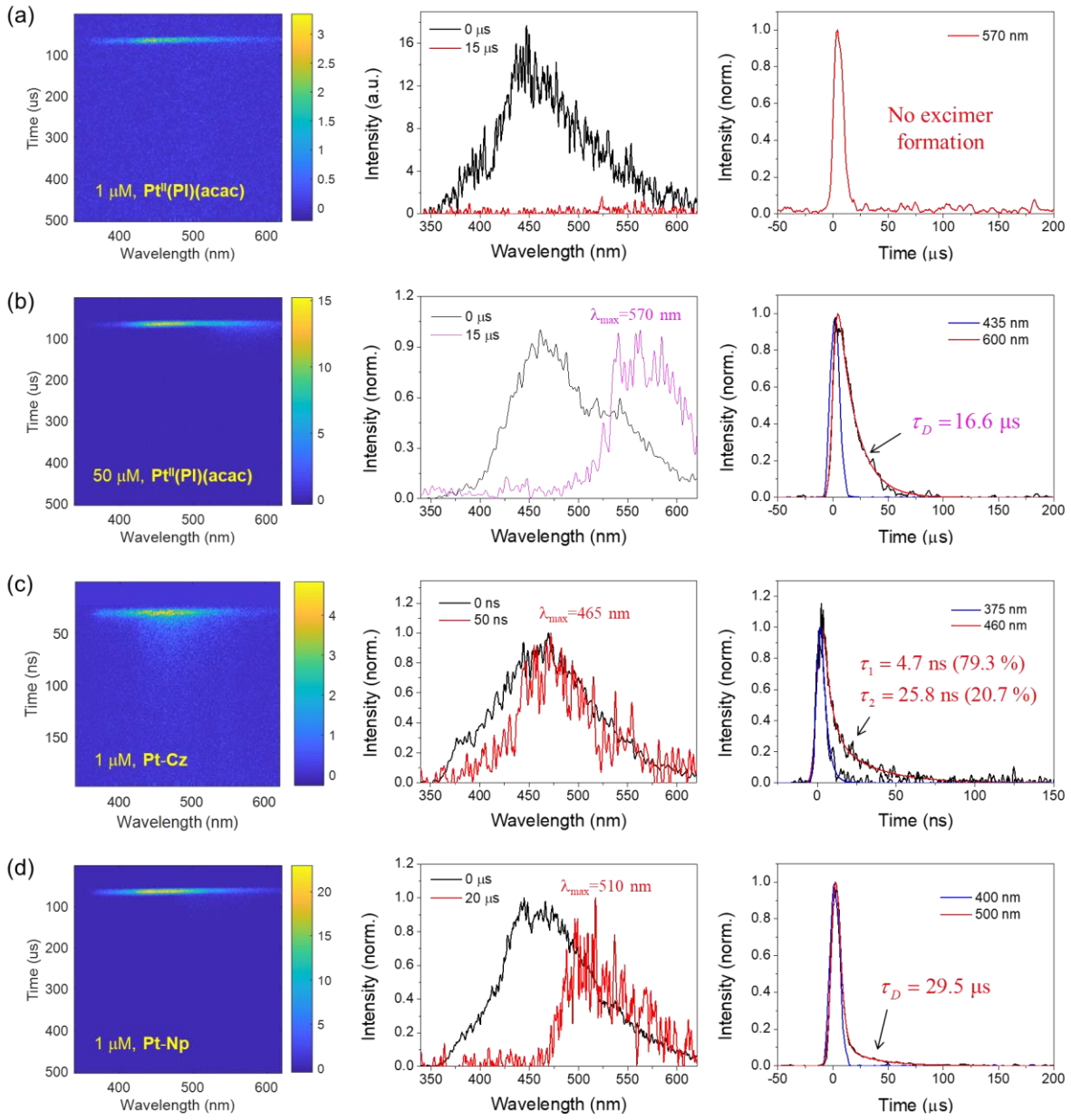

Supplementary Figure 11. Time-resolved photoluminescence (TRPL) analysis of Pt(II) complexes. TRPL spectra (raw contour images, left) of (a) Pt^{II}(PI)(acac) (1 μM), (b) Pt^{II}(PI)(acac) (50 μM), (c) Pt-Cz (1 μM), and (d) Pt-Np (1 μM) in DCM. The vertical color bar indicates PL intensity in counts per second (cps). Two representative TRPL spectra (middle) and time profiles in the 400–500 nm range (right) are shown. Multi-exponential fitting results of the TRPL profiles are summarized in Supplementary Table 6.

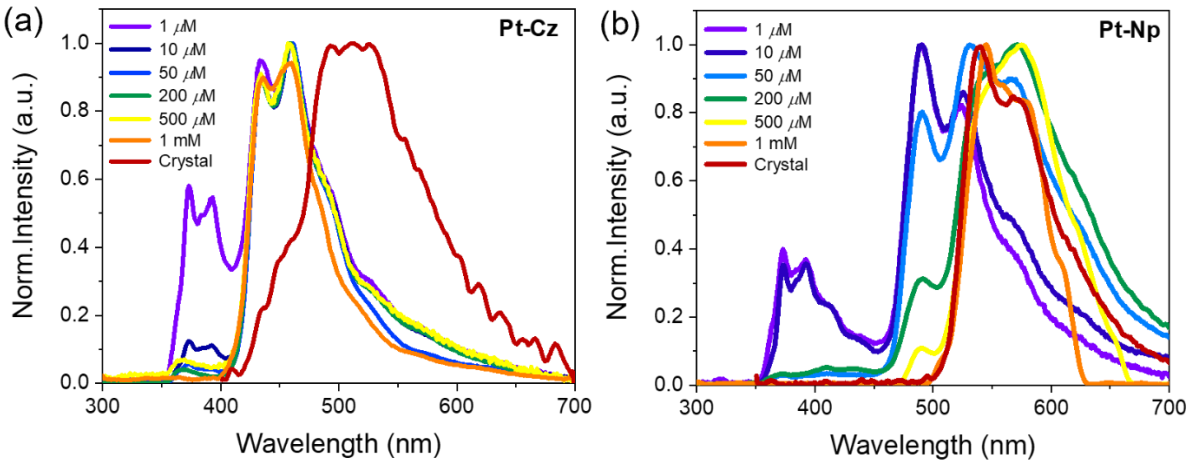

Supplementary Figure 12. Concentration-dependent and solid-state emission of Pt(II) complexes. Steady-state emission spectra of (a) Pt-Cz and (b) Pt-Np recorded over a wide concentration range (1 μM to 1 mM in DCM) in solution, as well as in the crystalline state.

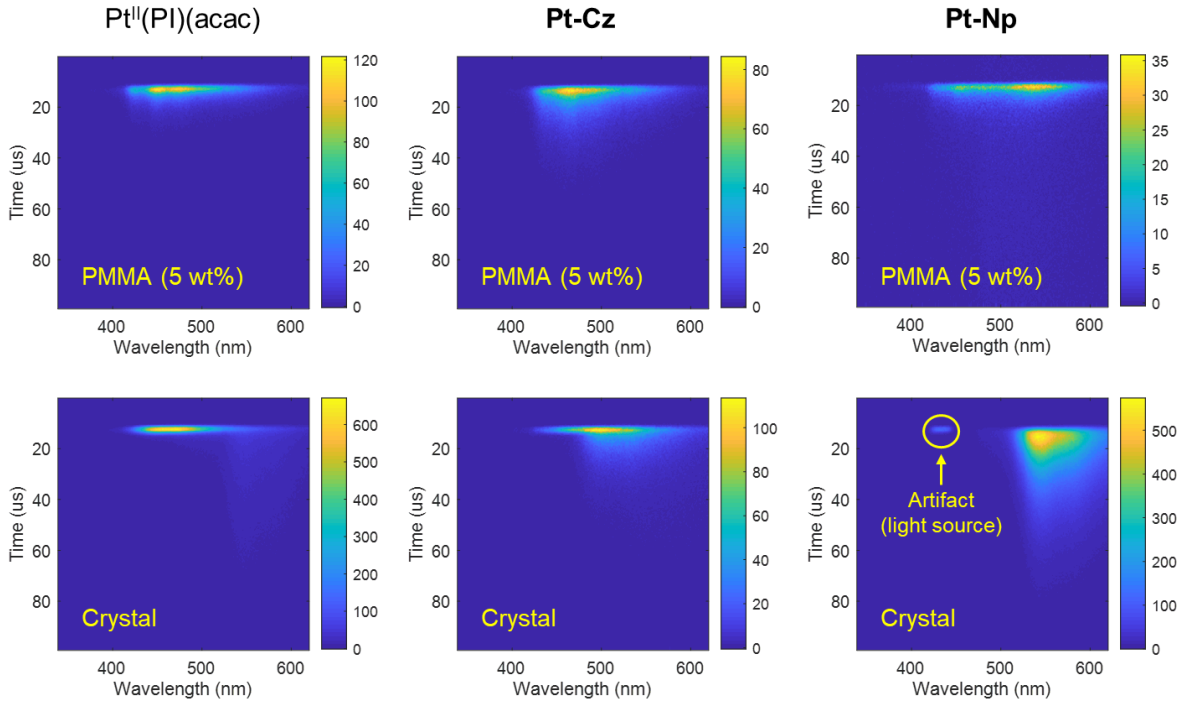

Supplementary Figure 13. Time-resolved photoluminescence (TRPL) of Pt(II) complexes in solid-state environments. TRPL spectra (raw contour images) of Pt^{II}(PI)(acac), Pt-Cz, and Pt-Np in PMMA films (5 wt%, top) and in their crystalline forms (bottom). The vertical color bar represents PL intensity in counts per second (cps).

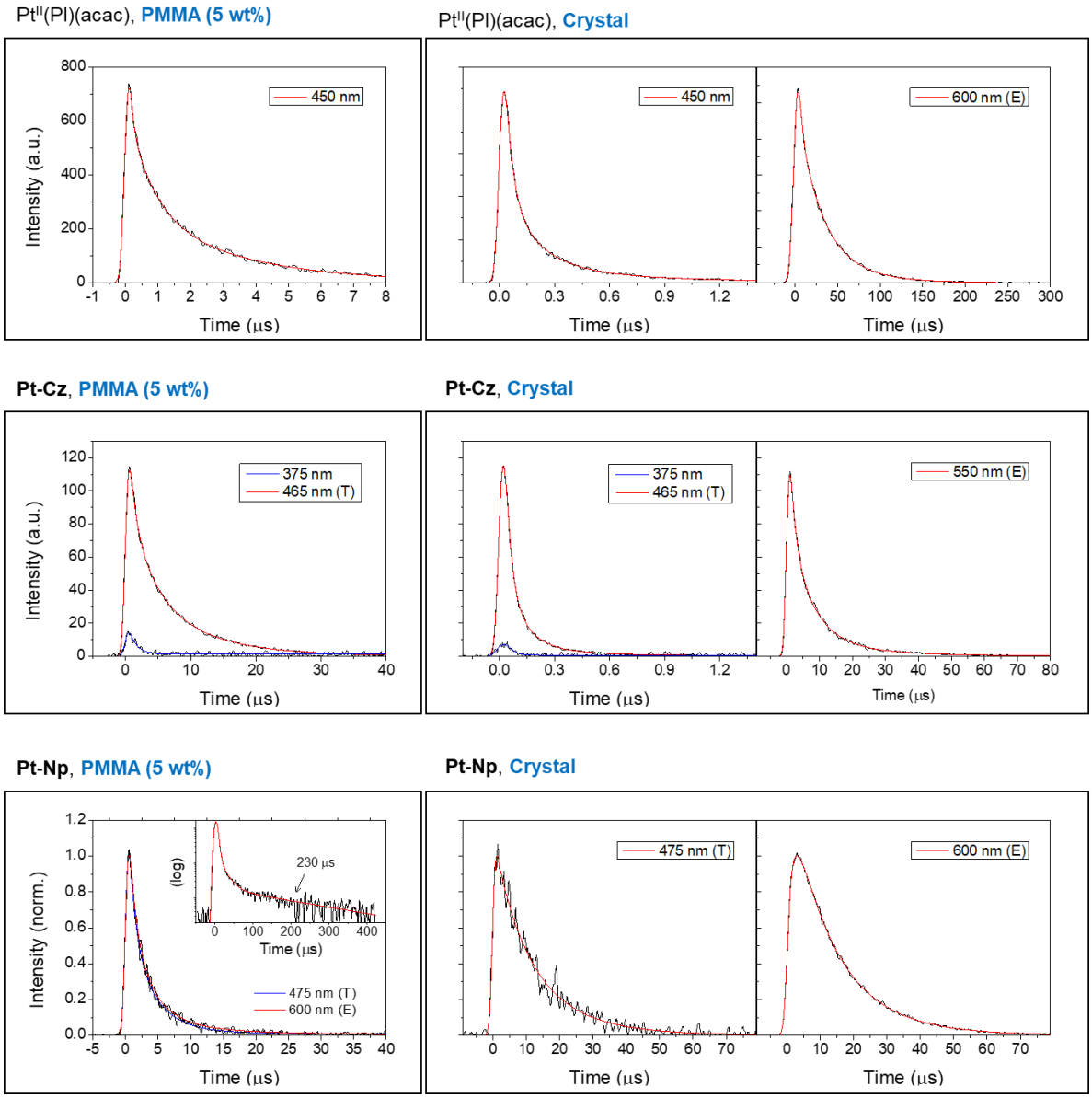

Supplementary Figure 14. Time-resolved photoluminescence (TRPL) profiles of Pt(II) complexes in solid-state environments. TRPL profiles of Pt^{II}(PI)(acac), Pt-Cz, and Pt-Np in PMMA films (5 wt%) and in their crystalline forms. In the legend, T denotes TTET (^{3}LC) and E denotes excimer emission.

Supplementary Table 6. Multiexponential fitting results for the TRPL profiles of Pt^{II}(PI)(acac), Pt-Cz, and Pt-Np in DCM. In the detection wavelength (λ_{em}) column, the symbols T and E in parentheses denote TTET (^{3}LC) and excimer, respectively.

Sample	Conc. (μM)	λ_{em} (nm)	A_1 (%)	t_1 (μs)	A_2 (%)	t_2 (ms)
Pt^{II}(PI)(acac)	1	450	100	1.1		
Pt-Cz	1	375	100	<IRF		
		465 (T)	79.3	4.7 ns	20.7	25.8 ns
Pt-Np	1	400	100	< IRF [a]		
		550 (T)	96.0	< IRF	4.0	29.5
Pt^{II}(PI)(acac)	50	435	100	< IRF		
		600 (E)			100	16.6
Pt-Cz	50	375	91.6	< IRF	8.4	23.9 ns
		465 (T)			100	24.2 ns
Pt-Np	50	475 (T)			100	>100 [b]
		600 (E)	–36.5 [c]	17.8	63.5	>100

a) This component is limited by the time-resolution (IRF width) of the streak-scope setup. b) The decay component longer than 100 μs is limited by the Ar-purging condition. c) Negative amplitude indicates a rise component.

Supplementary Table 7. Multiexponential fitting results for the TRPL profiles of Pt^{II}(PI)(acac), Pt-Cz, and Pt-Np in PMMA (5 wt%) and crystalline form. In the detection wavelength (λ_{em}) column, the symbols T and E in parentheses denote TTET (^{3}LC) and excimer, respectively.

Sample	Phase	λ_{em} (nm)	A_1 (%)	t_1 (μs)	A_2 (%)	t_2 (μs)	A_3 (%)	t_3 (μs)
Pt^{II}(PI)(acac)	PMMA	450	53.8	1.01	46.2	3.41		
	Crystal	450	69.9	38 ns	25.3	176 ns	4.8	0.70
		600 (E)	79.4	1.14	16.9	27.8	3.8	52.2
Pt-Cz	PMMA	375	94.6	<IRF [a]	5.4	>5		
		465 (T)	40.9	0.89	37.1	4.06	22.1	10.4
	Crystal	375	96.6	<IRF	3.4	>0.5		
		465 (T)	77.1	30.6 ns	21.5	0.12	1.3	0.72
		550 (E)	48.4	1.50	46.9	6.90	4.6	26.2
Pt-Np	PMMA	475 (T)	57.4	1.17	39.1	3.84	3.5	19.4
		600 (T)	54.1	0.87	44.4	3.54	1.4 (0.3)	34.8 (230) [b]
	Crystal	475 (T)	48.3	0.24	30.8	9.1	20.9	16.7
		600 (E)	–33.8 [c]	1.82	36.8	10.0	29.4	16.0

a) This component is limited by the time-resolution (IRF width) of the streak-scope setup. b) at 600 nm, a negligible decay component of 230 μs (A = 0.3%) was found in the extended time window of 500 μs. c) Negative amplitude indicates a rise component.

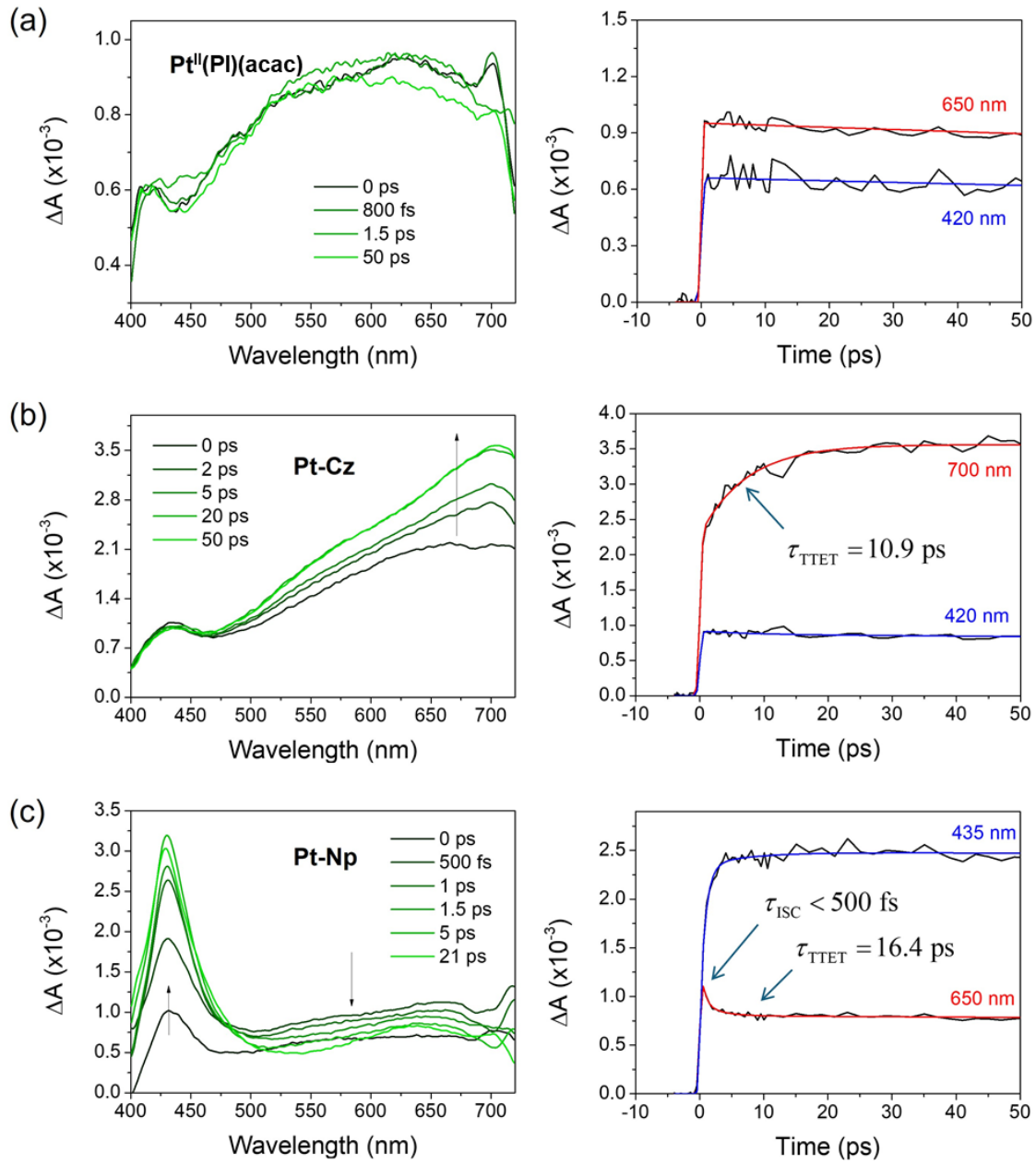

Supplementary Figure 15. Femtosecond transient absorption (TA) analysis of Pt(II) complexes. Femtosecond TA spectra of Pt^{II}(PI)(acac), Pt-Cz, and Pt-Np in DCM (50 μM). Two representative TA time-profiles, recorded on the blue and red sides of the spectra, are presented with guiding solid lines.

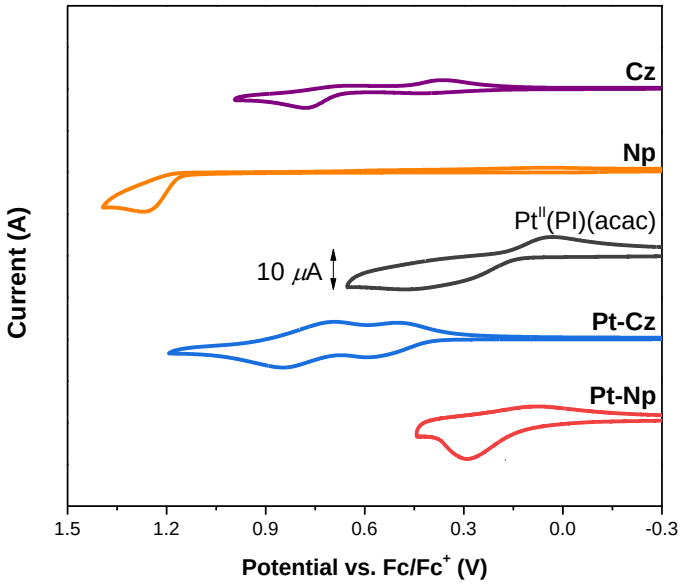

Supplementary Figure 16. Electrochemical oxidation behavior of ligands and Pt(II) complexes. Cyclic voltammograms of carbazole (Cz), naphthalene (Np), and Pt(II) complexes (1 mM) showing the oxidation region, measured in DCM with 0.1 M TBAP as the supporting electrolyte. Scan rate: 100 mV s^{-1}.

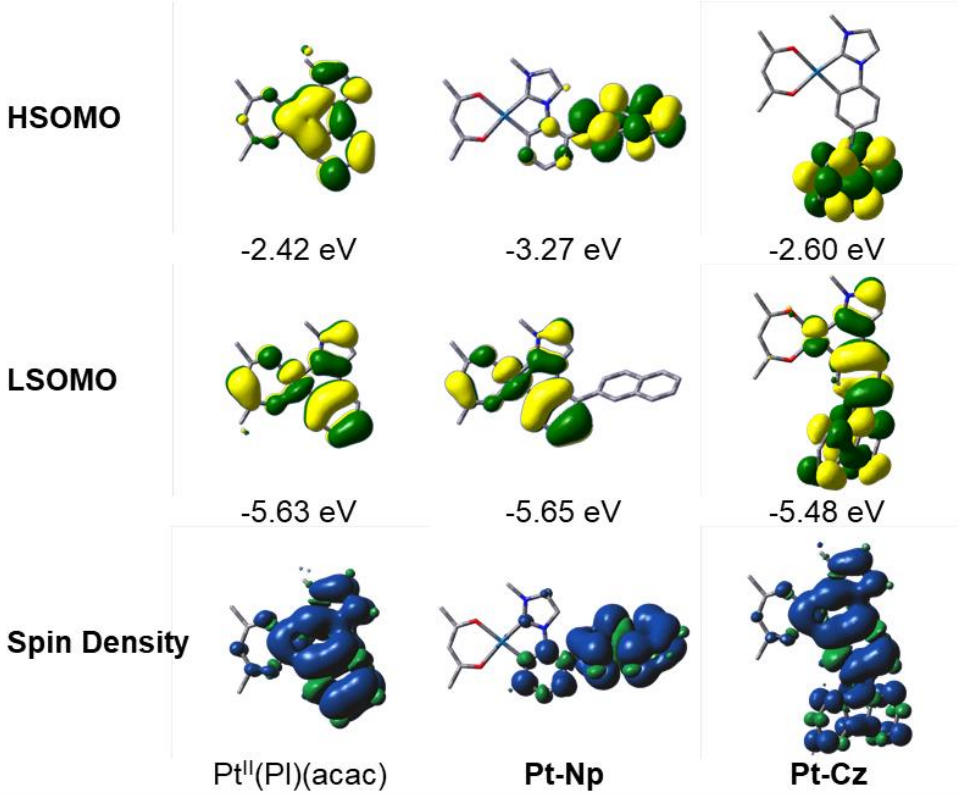

Supplementary Figure 17. Optimized triplet-state geometries and electronic properties of Pt(II) complexes. Optimized triplet excited-state structures, highest and lowest singly occupied molecular orbitals (HSOMO and LSOMO), and spin density distributions of the Pt(II) complexes.

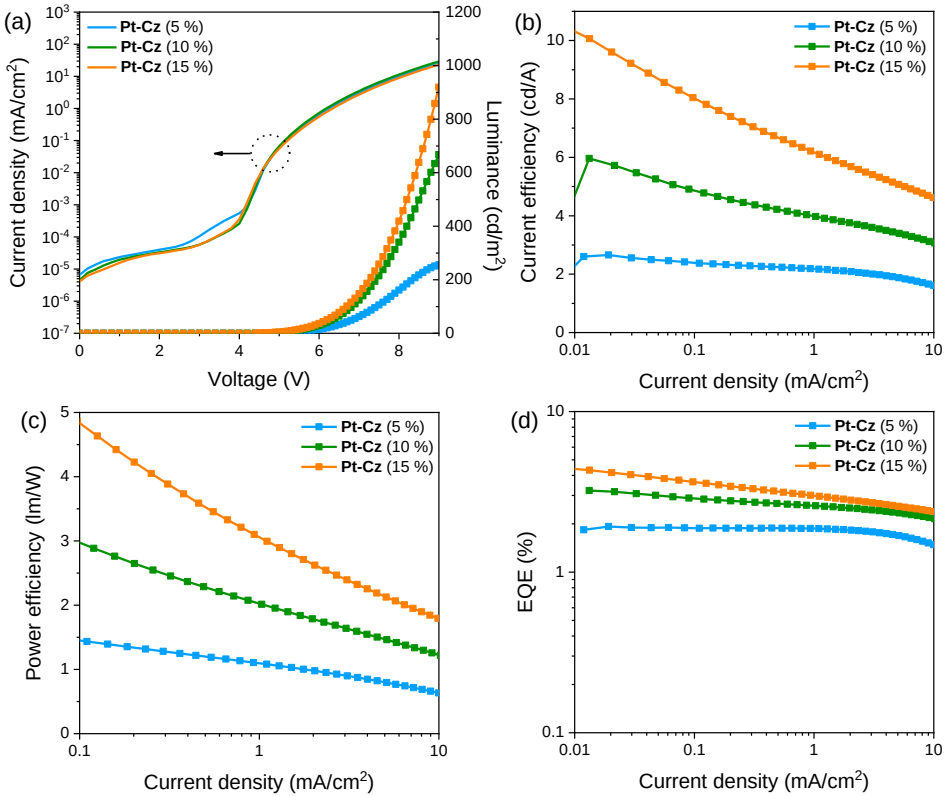

Supplementary Figure 18. Device performance of Pt-Cz-doped OLEDs at varying doping concentrations (5–15%). (a) Current density–voltage–luminance (*J–V–L*) characteristics, (b) current efficiency (CE) versus current density, (c) power efficiency (PE) versus current density, and (d) external quantum efficiency (EQE) versus current density.

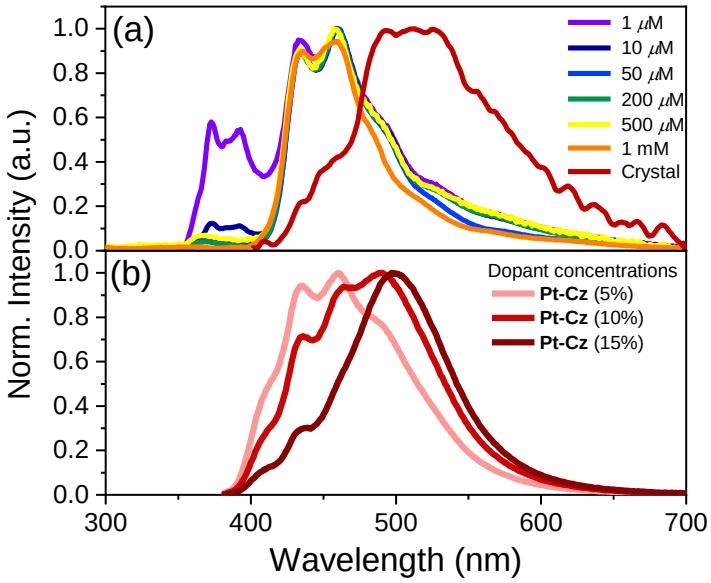

Supplementary Figure 19. Photoluminescence and electroluminescence characteristics of Pt-Cz. (a) Steady-state emission spectra of Pt-Cz measured across various solution concentrations (1 μM to 1 mM in DCM) and in its crystalline form. (b) Electroluminescence spectra of Pt-Cz-doped devices with different doping concentrations (5–15%).

Supplementary Table 8. Device characteristics of PhOLEDs using Pt-Cz as dopant

Device	Voltage[a)] (V)	EQE[b)] (%)	CE[b)] (cd/A)	PE[b)] (lm/W)	CIE[c)]	λ_{max}[c)] (nm)
Cz (5%)	4.90	1.92	2.66	1.78	(0.161, 0.175)	460
Cz (10%)	4.65	3.22	5.96	4.07	(0.168, 0.248)	491
Cz (15%)	4.55	4.44	10.53	7.52	(0.184, 0.361)	497

a) @ 1 cd/m^2. b) max values. c) @ 5 V.

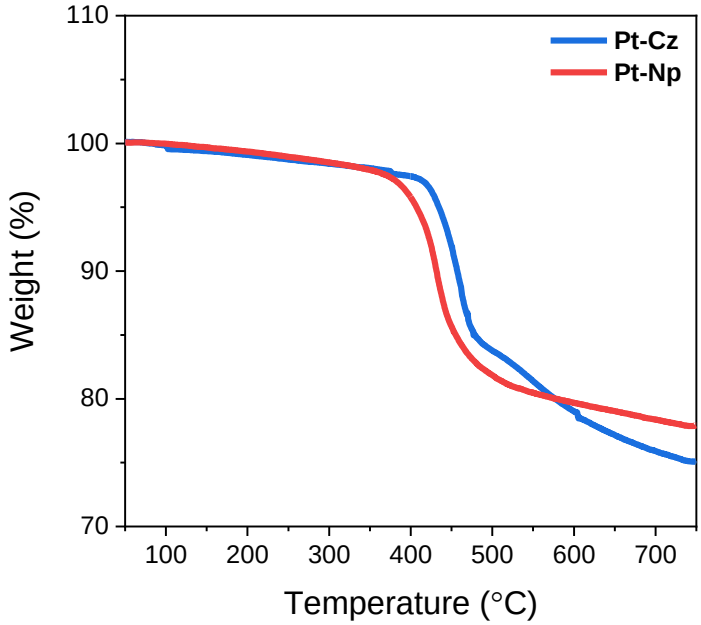

Supplementary Figure 20. Thermal stability of Pt(II) complexes. TGA curves and corresponding thermal parameters of the Pt(II) complexes. Measurements were performed using a PerkinElmer TGA 4000 instrument over a temperature range of 30–800 °C under a nitrogen flow, with a heating rate of 30 °C min^{-1}.

Supplementary References

[1] Atwood, J. L., Davies, J. E. D., MacNicol, D. D. & Vogtle, F. *In Comprehensive supramolecular chemistry* Pergamon: Oxford (1996).

[2] Kim, S.-Y. et al. Photoinduced electron and hole transfers in carbazole dendrimers with heteroleptic Ir-complex cores. *Phys. Chem. Chem. Phys.* **20**, 27585−27591 (2018). DOI: 10.1039/C8CP04971H